

# Experimental Determination of the Pressure Dependence of the Thermal Diffusivity of Teflon, Sodium Chloride, Quartz, and Silica

SUSAN WERNER KIEFFER

*Department of Geology, University of California, Los Angeles, California 90024*

IVAN C. GETTING AND GEORGE C. KENNEDY

*Institute of Geophysics, University of California, Los Angeles, California 90024*

The thermal diffusivity of Teflon, sodium chloride, quartz, and silica glass was measured at 40°C to pressures of 35, 18, 30, and 36 kbar, respectively. A transient line source method was modified for use in a piston-cylinder high-pressure cell. Pressure gradients were determined by experiments with bismuth foils. The pressure dependence of the thermal diffusivity at 40°C for the substances studied may be represented as follows ( $\kappa$  in square centimeters per second,  $P$  in kilobars): for the low-pressure phases of Teflon, Teflon I-II,  $P < 5.5$  kbar,  $\kappa = 0.0012 + 3.6 \times 10^{-5}P$ ; for the high-pressure phase, Teflon III,  $5.5$  kbar  $< P < 35$  kbar,  $\kappa = 0.0012 + 8.0 \times 10^{-5}P$ ; for polycrystalline halite,  $P < 18$  kbar,  $\kappa = 0.0031 + 9.5 \times 10^{-4}P$ ; for quartz, perpendicular to the  $c$  axis,  $P < 30$  kbar,  $\kappa = 0.031 + 5.3 \times 10^{-4}P$ ; for silica glass,  $P < 36$  kbar,  $\kappa = 0.0068 - 6.7 \times 10^{-5}P$ . The diffusivity of silica glass decreases with pressure, in contrast to the diffusivity of its crystalline counterpart, quartz, which increases with pressure. In addition to the diffusivity the thermal conductivity of Teflon was determined by measuring the power applied to the heater wire. The thermal conductivity of a Teflon I-II mixture is approximately constant at 0.0075–0.0078 cal/cm s °K to 5.5 kbar. Above 5.5 kbar the conductivity of Teflon III is given by  $K = 0.0062 + 4.0 \times 10^{-5}P$ . The specific heat of Teflon decreases with pressure and decreases discontinuously by 15% across the Teflon II-III phase change, in good agreement with the decrease predicted from thermal expansion and compressibility data.

## INTRODUCTION

There are only a few reported data in the literature on the variation of the thermal conductivity or diffusivity of minerals with pressure [Bridgman, 1924; Fujisawa *et al.*, 1968; Schloessin and Dvorak, 1972]. We report here new thermal diffusivity ( $\kappa$ ) data for Teflon, sodium chloride, quartz, and silica glass and thermal conductivity ( $K$ ) and specific heat ( $c$ ) data for Teflon. These substances were chosen for measurements for a variety of reasons: (1) Teflon, as a material that is commonly used in pressure cells, as a material for which values had been published [Andersson and Bäckström, 1972], and as a material with phase transitions in the range of pressures attainable [Pistorius, 1964]; (2) sodium chloride (polycrystalline), as a crystalline substance whose atomic structure allows theoretical calculations of the thermal properties [e.g., Mooney and Steg, 1969]; (3) quartz, as a framework silicate representative of minerals in the earth's crust; and (4) silica glass, as an amorphous material for comparison with its crystalline counterpart, quartz.

## THEORY: LINE SOURCE METHOD

We modified the transient line source method first proposed by Jaeger [1959] and later developed by Jaeger and Sass [1964] for application to a piston-cylinder high-pressure cell. In this method a thin linear heater serves as the heat source; the temperature rise ( $v$ ) above ambient is recorded as a function of time ( $t$ ) at a known distance from the heater. The thermal diffusivity and conductivity may be determined from this temperature-time ( $v$ - $t$ ) curve and a knowledge of the power output of the heater. Many advantages of the method as used for work at 1-atm pressure were listed by Jaeger and Sass [1964]. In addition, the method has the following advantages for high-pressure work: (1) the diffusivity and conductivity are both

determined, either allowing the specific heat to be determined through  $c = K/\rho\kappa$  or providing a consistency check if the specific heat is known; (2) the early part of the temperature-time history may be used, thus minimizing violations of boundary conditions which are in general difficult to maintain in the pressure apparatus; (3) thermal properties are measured in a single plane, perpendicular to the line source; (4) sample design is amenable to the inherent pressure vessel geometry; (5) sample size maximized so that experimental errors due to the finite size of the heater wire and the thermocouple are minimized; (6) sample preparation, while it is not trivial, is relatively simple. The main disadvantage of the method is that data reduction is complex.

An inherent difficulty with the application of most methods of simultaneously measuring the thermal diffusivity and conductivity to high pressure is in providing an accurate description of the boundary conditions on the sample. The original line source method of Jaeger and Sass [1964] applies to a sample which is perfectly insulated or has only small heat losses. It is not possible to insulate a mineral sample (which is itself a good insulator) in a high-pressure vessel. We performed several experiments which showed that the assumptions of perfect insulation or small heat losses from the sample are not even approximated at high pressure. We therefore decided to make the cylindrical surface of the sample as nearly isothermal as possible by placing the sample in contact with good thermal conductors. The following theory, then, is a modification of the Jaeger and Sass [1964] theory to this boundary condition.

An infinitely long circular cylinder  $0 < r \leq a$  (or equivalently, one which is perfectly insulated at the ends so that the axial flux is zero,  $dv/dz = 0$ ) is assumed to have a thermal conductivity  $K$ , density  $\rho$ , specific heat  $c$ , and thermal diffusivity  $\kappa = K/\rho c$ .  $K$ ,  $\kappa$ ,  $\rho$ , and  $c$  are assumed to be independent of temperature. The initial differential temperature between the

cylinder and its surroundings ( $v$ ) is assumed to be zero ( $v = v_0(r) = 0$ ) at time zero ( $t = 0$ ). The outer surface ( $r = a$ ) is assumed to be an isothermal surface ( $v = v(a) = 0$  for all  $t > 0$ ). For all time  $t > 0$ , there is a line source of infinitely small diameter parallel to the axis through the point whose polar coordinates are  $(r', 0)$ . This source emits heat at the constant rate  $Q$  per unit length per unit time.

The basic equation of heat conduction in cylindrical coordinates is

$$\kappa \left[ \frac{\partial^2 v}{\partial r^2} + \frac{1}{r} \frac{\partial v}{\partial r} + \frac{1}{r^2} \frac{\partial^2 v}{\partial \theta^2} \right] - \frac{\partial v}{\partial t} = 0 \quad (1)$$

The differential temperature  $v$  (henceforth referred to simply as the temperature) at the point  $(r, \theta)$  at time  $t$  ( $t > 0$ ) is obtained by applying, successively, a Laplace transform, the addition theorem, the inversion theorem, and the theory of residues, or by direct integration of the Green's function [Carslaw and Jaeger, 1959, p. 385]. For a line source and the thermocouple at equal distances,  $r' = r$ , the solution is

$$\frac{\pi K v(r)}{Q} = \frac{1}{2} \left\{ -\ln \left( \frac{r}{a} \right) + \ln \frac{[1 + (r/a)^2]}{2} \right\} - \sum_{n=0}^{\infty} \epsilon_n \cos n\theta \sum_{m=0}^{\infty} \frac{\exp [-\kappa \alpha_{n,m}^2 t/a^2] J_n^2[\alpha_{n,m}(r/a)]}{(\alpha_{n,m}^2/a^2) J_n'^2(\alpha_{n,m})} \quad (2)$$

where  $Q$  is the heat emission per unit length,  $K$  is the conductivity,  $\kappa$  is the diffusivity,  $r$  is the radius to the heater and thermocouple (assumed equal),  $a$  is the cylinder radius,  $\epsilon_n = 1$  for all  $n = 0$ ,  $\epsilon_n = 2$  for  $n \geq 1$ , and  $\alpha_{n,m}$  are the positive roots of  $J_n'(a) = 0$ . This solution consists of two terms: the first, a steady state term; the second, a transient term which is a complicated function of the sample geometry.

#### EXPERIMENTAL PROCEDURE AND DATA REDUCTION

The experiments were conducted in an end-loaded piston-cylinder apparatus to a maximum pressure of 35 kbar. The initial temperature ( $T_0$ ) was room temperature (about 27°C). The high-pressure cell which contained the sample was placed in a large pressure vessel (3.18 cm (1¼ inches) in bore diameter by 15.24 cm (6 inches)) in length. The outside of the vessel was cooled by continuously circulating water.

The high-pressure cell is shown in detail in Figure 1. The sample (5.08 cm (2 inches) in length, 1.27 cm (½ inch) in diameter) contained two diametrically opposing slots, passing through the points  $(r, 0)$  and  $(r, \pi)$ ;  $r$  was generally chosen to be 0.7 of the sample radius. The heater wire and thermocouple (Chromel-Alumel) were placed in opposed slots. For Teflon samples the wires were packed into the slots with Teflon; glass was melted into the slots of quartz and glass samples; and sodium chloride was packed into the slots of the sodium chloride sample. The four wires from the heater and thermocouple were brought out from the high-pressure environment through a four-hole ceramic tube at the top of the assembly.

The cell was designed to achieve two conditions: (1) the desired thermal boundary conditions on the sides and ends of the cylinder, and (2) a condition of uniform stress distribution. The sample was surrounded in the radial direction by good conductors which coupled it thermally to the pressure vessel and cooling system. Such thermal coupling gave a reasonable approximation to the boundary condition of the cylinder surface that the differential temperature remain zero ( $v(a) = 0$  for all  $t > 0$ ). Silver was chosen as the material to be placed

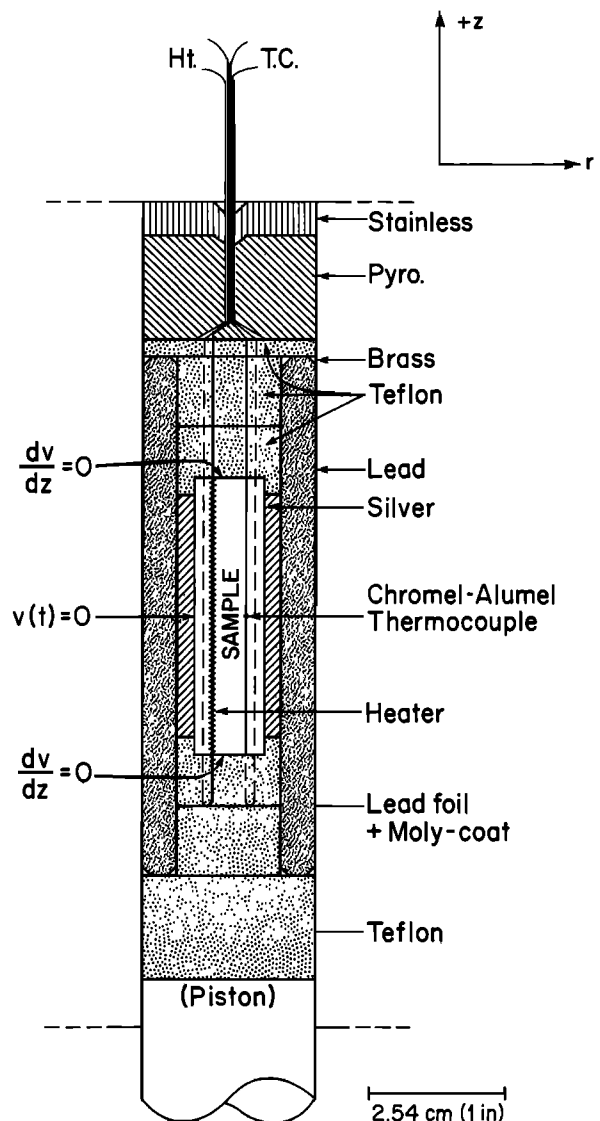


Fig. 1. High-pressure cell for measurement of  $\kappa$ ,  $K$ , and  $\rho c$  by the line source method.

immediately in contact with the sample because of its high thermal conductivity. To assure reasonable stress distribution, however, a weaker bushing of lead (a slightly poorer conductor) was placed outside the sample over a substantial length of the cell. An insulator, Teflon, was placed at the ends of the sample to give a reasonable approximation to the boundary condition that the axial heat flux be zero ( $dv/dz = 0$ ).

Ideally, the sample environment should be hydrostatic. This condition is impossible to attain in a solid medium pressure apparatus because of the finite shear strengths of the various cell components. Weak materials (lead and Teflon) were used wherever possible in order to minimize shear stresses.

Stress distribution in the cell was studied in a separate experiment of geometry similar to the thermal measurement assembly. Bismuth foils were placed at the ends of a Teflon sample, as is shown in Figure 2. As the pressure was increased and decreased through two cycles, the Bi I-II and II-I transitions in each foil were observed by monitoring electrical resistance. Although these foils are expected to respond most sensitively to the axial component of stress, we have taken them to be reasonable indicators of pressure. On compression, the Bi

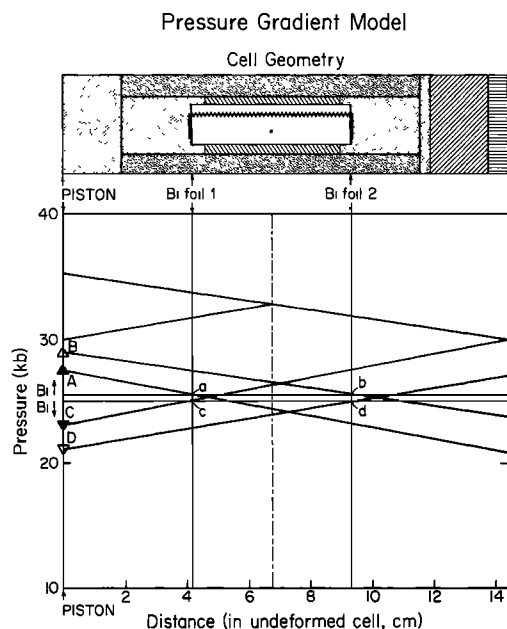


Fig. 2. Pressure gradients in the high-pressure cell. Data points A, B, C, and D indicate applied pressure at which the bismuth I-II transition (A and B) and the II-I transition (C and D) were observed at the two foils. Closed triangles represent transitions in foil 1; open triangles, foil 2. In this plot, linear pressure distributions are constructed to pass through these points and the corresponding locations (*a*, *b*, *c*, and *d*) at which the transitions actually occurred. The top line shows the assumed pressure distribution at an applied pressure of 35.2 kbar; reduction of this applied pressure to 30.0 kbar is necessary to just reverse the pressure gradient at the center of the cell. Complete reversal of the gradients is not attained until the pressure is reduced to 23.0 kbar, coincident with point C.

I-II transition pressure was taken as 25.5 kbar [Heydemann, 1967]; the Bi II-I transition on decompression was assumed to be about 0.5 kbar lower [Davidson and Lee, 1964].

Upon compression the foil nearer the piston underwent the I-II transition at a pressure of 27.3 kbar applied to the piston; the more remote foil, at 28.8 kbar. On decompression the foil nearer the piston underwent the II-I transition at 23.0 kbar; the more distant foil, at 21.1 kbar. These values are symmetrically located about the true transition pressures to within 0.2 kbar for the foil nearer the piston and 0.6 kbar for the more distant. The departures from symmetry were of opposite signs at the two ends of the sample. The applied pressures at which the transitions took place implied an axial pressure gradient of 0.4 kbar/cm (1.2 kbar/inch) over the 5.08-cm (2.0 inches) initial length of the sample.

The thermocouple used in the thermal measurements was located at the midpoint of the sample's length. Thermal scaling of the experiment shows that during a typical run of 100-s duration the thermocouple history is most influenced by material within a distance slightly less than one cylinder diameter, that is, by material within 1.27 cm ( $\frac{1}{2}$  inch) of the thermocouple. Thus we estimate that the pressure variation within material which influences the experimental results is about 1 kbar. Since the pressure gradient is probably uniform in the central region, it is reasonable to assume that the pressure differences are largely self-compensating and that the thermal properties are averaged over  $\pm \frac{1}{2}$  kbar about the mean pressure.

In order to estimate the mean pressure at the center of the sample, diffusivity measurements were made on compression and decompression over several pressure ranges. The data for Teflon are shown in Figure 3a. Having observed the frictional

effects to be reasonably symmetrical in the bismuth experiments, we chose the midpoint of hysteresis loops as the pressure at the center of the sample. In the central region of the loop ( $\sim 7$  to  $\sim 27$  kbar) the correction is 2–3 kbar (Figure 3b). The ends of individual hysteresis loops are complicated by pressure gradient reversals. At the lower ends they are also complicated by phase changes in the Teflon. Data from these regions are not considered in determining friction corrections. On the 35-kbar excursion, complete pressure gradient reversal upon decompression appears to have occurred by 26 kbar (Figure 3a). This value is in reasonable agreement with the value required to reverse the gradient in the vicinity of the sample center (from the linear model of Figure 2).

The temperature-time ( $v$ - $t$ ) history of the thermocouple was recorded (generally for about 2 min) on a strip chart recorder. Data reduction was accomplished by using the method of Jaeger [1959] using only the early part of the temperature-time curve, typically the first 30 s to 1 min. The theoretical solution (2) of the temperature-time curve is of the form

$$v(t) = A(K, \kappa)f(\kappa t/a^2) \quad (3)$$

where  $A$  is a constant depending on  $K$  and  $\kappa$ . From this, it follows that

$$\frac{v(nt)}{v(t)} = \frac{f(n\kappa t/a^2)}{f(\kappa t/a^2)} \quad (4)$$

where  $n$  is a positive number, generally taken to be an integer. With the aid of a theoretical curve or table of the function  $f(n\kappa t/a^2)/f(\kappa t/a^2)$  a value of  $\kappa t/a^2$  can be found from an experimental value of  $v(nt)/v(t)$  [Jaeger, 1959].

In practice, convenient units of time  $t = t_0$  and  $n$  are chosen, e.g.,  $t_0 = 2$  s,  $n = 2$ . Values of  $v(mt_0)$  are read from the strip chart at times  $mt_0$ ,  $m = 1, 2, \dots$ . The ratios  $v(nmt_0)/v(mt_0)$  are calculated and compared to tables of the function

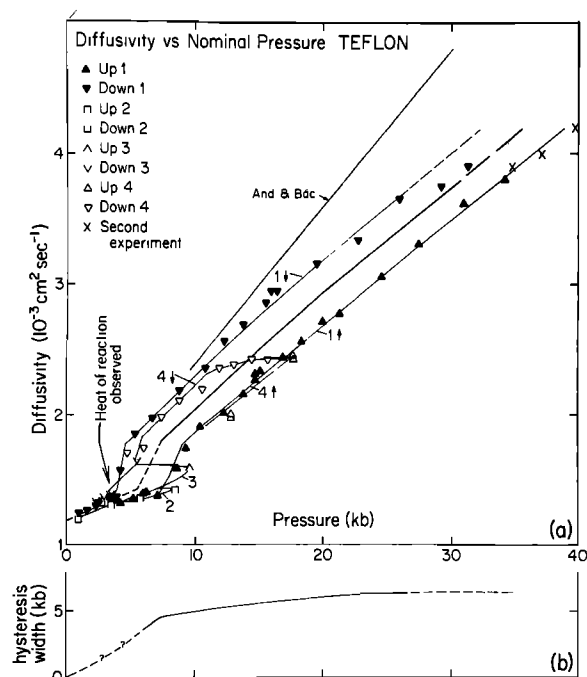


Fig. 3. (a) Diffusivity of Teflon versus pressure. Four hysteresis loops are shown. The center (heavy) line represents the midpoint values. The light line shows the relative values of Andersson and Bäckström [1972] normalized to our 1-bar value. (b) Hysteresis loop width versus pressure.

$f(n\kappa t/a^2)/f(\kappa t/a^2)$  generated from (2). From these tables a value of  $\kappa$  is determined for each ratio. In theory, each ratio  $v(nmt_0)/v(mt_0)$  gives the same value of  $\kappa$ , or values which agree within experimental error. In practice, we observed systematic drift of the values in all but the earliest parts of the  $v$ - $t$  curves, an indication that the theory did not perfectly represent the experimental situation. In these cases we extrapolated the drifting values back to the nominal value at  $t = 0$ . When  $\kappa$  has been determined, the value of  $K$  can be found from (3) (if the heater power,  $Q$ , has been measured) by comparing the observed values of  $v(t)$  with the theoretical value  $A(K, \kappa)f(\kappa t/a^2)$ . From  $K$  and  $\kappa$  the specific heat can be determined from  $c = K/\rho\kappa$ .

The observed diffusivity values vary somewhat with variations in the power applied to the heater wire. Higher heater power causes a higher average temperature in the sample. We therefore expect the observed values to reflect the temperature dependence of the diffusivity. This is indeed the case. For Teflon, higher values of diffusivity were measured at larger power outputs (e.g., a factor of 2 increase in power applied to the heater caused an increase of average diffusivity of about 10%). The published values of diffusivity of Teflon do indeed increase with temperature in the range 30°C–60°C [Shelley and Huber, 1968]. For quartz the diffusivity generally decreased slightly with applied power, as would be expected from the temperature dependence of the thermal conductivity [Clark, 1966, p. 466], but the dependence was slight. The diffusivity of glass did not vary with changes of a factor of 2 in applied power. No data were obtained on the power dependence of diffusivity of NaCl because of experimental problems. In order to minimize this temperature effect we used the minimum power required to give a resolvable  $v$ - $t$  curve for data reduction. The measured values of diffusivity are appropriate to a temperature averaged over the sample volume for the duration of the experiment. The value of temperature which we specify for our measurements is the highest temperature attained at the thermocouple during the duration of the experiments. Actual temperatures attained in the material between the heater wire and the thermocouple at the end of the experiment would have been slightly higher, but the value specified is probably a reasonable approximation to the mean temperature of the sample integrated over the duration of the experiment.

Because of the difficulty of the experiments we wished to determine the diffusivity and conductivity of a sample for which the values were previously known. After consideration of previously published data on diffusivity and conductivity of

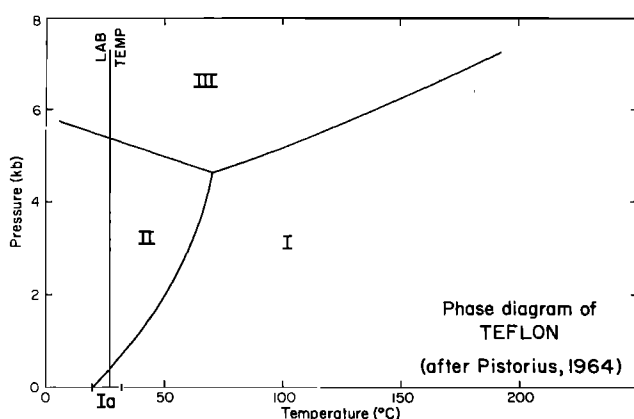


Fig. 4. Phase diagram of Teflon (polytetrafluoroethylene).

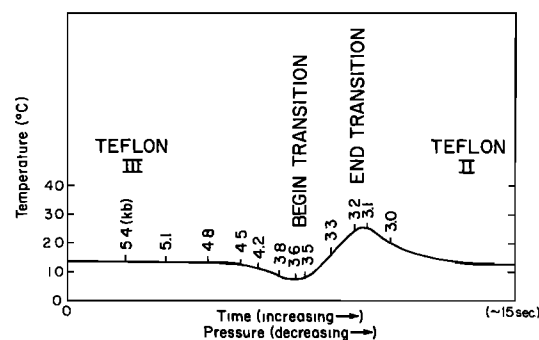


Fig. 5. Heat of reaction of the Teflon III–II phase change recorded as the pressure was decreased through the phase change region. Values of applied pressure during the decompression (not corrected for friction) are recorded beside the curve.

rocks, minerals, and polymers, we chose Teflon as the substance for use for our initial samples because (1) diffusivity and conductivity values for Teflon with small experimental uncertainties had been published by Andersson and Bäckström [1972]; (2) Teflon is commonly used in laboratory pressure cells, and knowledge of its thermal conductivity would aid in designing experiments; and (3) Teflon is easily machinable and therefore easy to use for developmental experiments.

## RESULTS

**Teflon.** Teflon shows several kinds of phase transitions (Figure 4) [Pistorius, 1964; Shelley and Huber, 1968]. At 1-bar pressure there is a strong first-order thermodynamic transition at 20°C (Teflon II–Ia in Figure 4; [Rigby and Bunn, 1949]). This transition is believed to be a screw dislocation, order-disorder transformation, in which the helical form of the polymer chain changes [Shelley and Huber, 1968]. At 30°C a transition (Teflon Ia–I in Figure 4) occurs as the polymer chain unwinds. The high-pressure data of Pistorius [1964] show a high-pressure phase, Teflon III, stable above about 5 kbar. These data show the Teflon I–II–III phase boundaries but do not resolve the I–Ia transition at high pressure.

Data in the literature regarding the behavior of the thermal diffusivity and conductivity across the phase boundaries are inconsistent. The 1-atm data of Kirichenko *et al.* [1964] and Ozawa and Kanari [1967] do not show discontinuities at the II–I and I–Ia transitions; the data of Shelley and Huber [1968] clearly resolve the transitions and show large variations in diffusivity through the transitions. The pressure data on diffusivity of Andersson and Bäckström [1972] do not resolve the II–III transition.

Our experimental diffusivity data for Teflon are shown in Figure 3. Below 5.5 kbar the diffusivity is given by  $\kappa(\text{cm}^2 \text{s}^{-1}) = 0.0012 + 3.6 \times 10^{-5} P(\text{kbar})$  at average temperature 40°C. The nominal value of the diffusivity extrapolated to 1 bar is  $0.0012 \text{ cm}^2 \text{ s}^{-1}$ . Although pressure uncertainties in a piston-cylinder apparatus are relatively large at pressures of a few kilobars, so that we could not resolve a phase change in this range of pressure, it is probable that the low-pressure data apply to a mixture of Teflon I and II, in which the proportion of Teflon II present increases with increasing pressure.

The diffusivity is discontinuous across the Teflon II–III phase boundary. The transition occurred gradually in the high-pressure cell at pressures between about 5 and 8 kbar. Although we did not see any evidence of the I–II transition at low pressures, the heat of reaction of the II–III phase transition was clearly recorded on the strip chart recorder by varia-

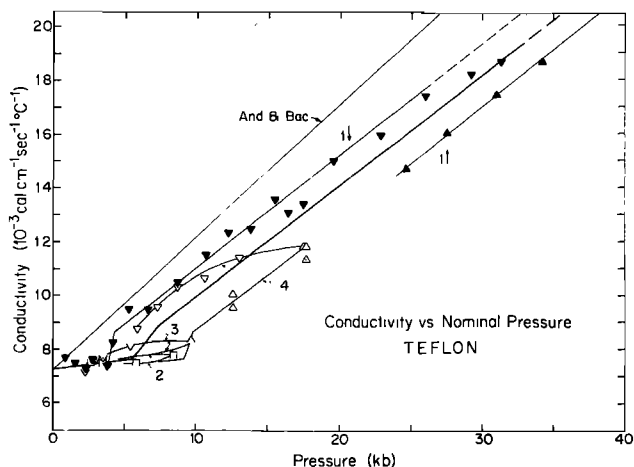


Fig. 6. Thermal conductivity of Teflon versus pressure. Same notation as for Figure 3.

tions in thermocouple temperature as the pressure was increased or decreased across the transition (Figure 5). The pressure at which the heat of reaction was recorded agrees well with the pressure at which the phase transition was reported (Figure 3) and with the measured discontinuity in the thermal diffusivity. The diffusivity has the value  $0.0020 \text{ cm}^2 \text{ s}^{-1}$  at 10 kbar and increases linearly to  $0.0045 \text{ cm}^2 \text{ s}^{-1}$  at 40 kbar. In this range the increase is  $8 \times 10^{-5} \text{ cm}^2 \text{ s}^{-1} \text{ kbar}^{-1}$ . The values of thermal diffusivity are somewhat lower than those reported by *Andersson and Bäckström* [1972], who did not resolve the II–III phase transition. It is possible that variations in the sample properties (degree of crystallinity, method of manufacture) account for the lack of agreement between the two sets of results, although the density of the samples used was nearly identical ( $2.15 \text{ g cm}^{-3}$  [Andersson and Bäckström, 1972],  $2.144 \text{ g cm}^{-3}$  (this paper)).

In order to determine the conductivity  $K$  from the diffusivity  $\kappa$  it is necessary to measure the power dissipated per unit length in the line source. Limited by the number of wires exiting from the cell, we were not able to measure this power in situ. Instead, the initial resistance of both the heater and its copper leads was measured before assembly into the pressure vessel. During the run the heater current and total resistance of the leads plus heater were measured. The copper leads inside the cell changed in resistance owing to the effect of pressure. *Bridgman* [1938] observed a 5% decrease in the resistance of copper from room pressure to 30 kbar. After this correction was applied to the

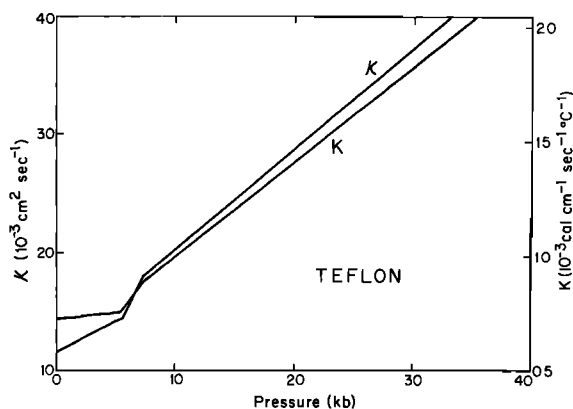


Fig. 7. Summary of thermal diffusivity and conductivity data for Teflon.

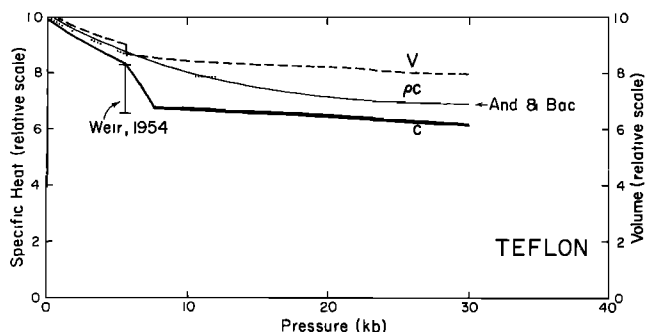


Fig. 8. Specific heat and volume of Teflon versus pressure.

pressurized length of copper leads, the final heater resistance was observed to vary from  $0.63 \Omega$  initially to  $0.50 \Omega$  at 35 kbar.

The thermal conductivity data obtained for Teflon are shown in Figure 6. Below 5.5 kbar the conductivity is approximately constant at  $K = 0.00075 \text{ cal cm}^{-1} \text{ s}^{-1} \text{ }^\circ\text{C}^{-1}$ ; the conductivity does increase slightly with pressure in this range, to a value of  $K = 0.00078 \text{ cal cm}^{-1} \text{ s}^{-1} \text{ }^\circ\text{C}^{-1}$  at 5.5 kbar. These values are attributed to a Teflon I–II mixture or to Teflon II. The conductivity is discontinuous across the Teflon II–III phase boundary. Extrapolated to 5.5 kbar, it has the value  $0.00088 \text{ cal cm}^{-1} \text{ s}^{-1} \text{ }^\circ\text{C}^{-1}$  and by 30 kbar increases to  $0.00187 \text{ cal cm}^{-1} \text{ s}^{-1} \text{ }^\circ\text{C}^{-1}$ . This increase in conductivity for Teflon III is  $5.5\% \text{ kbar}^{-1}$ , somewhat lower than the  $(7.6 \pm 0.8)\% \text{ kbar}^{-1}$  reported by *Andersson and Bäckström* [1972].

The experimental values for  $\kappa$  and  $K$  are summarized in Figure 7. From these values and *Bridgman's* [1948] compression data the specific heat was determined from  $c = K/\rho\kappa$  (Figure 8). The specific heat decreases nonlinearly by 17% from 0 to 5 kbar and decreases by 15% across the Teflon II–III phase change, in good agreement with the decrease across the phase change predicted by *Weir* [1954] from thermal expansion and compressibility data.

**Quartz.** The thermal diffusivity of single-crystal quartz was measured perpendicular to the  $c$  axis (Figure 9). Although two cycles of compression and decompression were measured, the data shown in Figure 9 are selected from only two traverses. Data from a smaller, interior hysteresis loop were badly scattered and are not shown. The hysteresis loop width obtained from the first compression and last decompression is

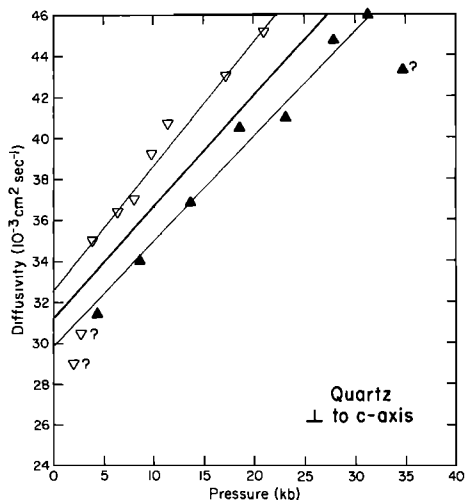


Fig. 9. Thermal diffusivity of quartz, perpendicular to the  $c$  axis, versus applied pressure.

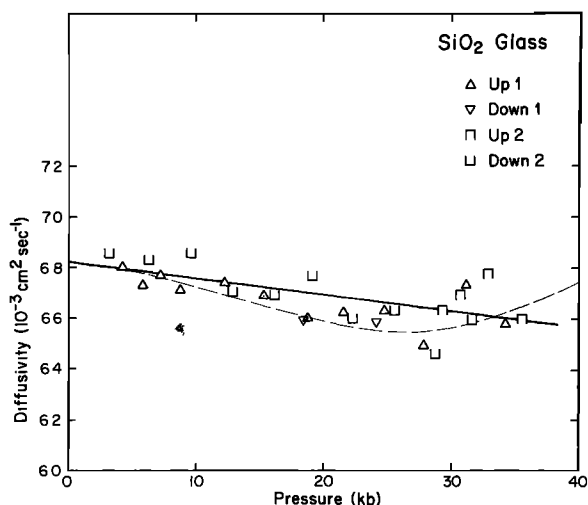


Fig. 10. Thermal diffusivity of silica glass versus pressure. Two hysteresis loops are represented. Solid line represents least squares linear fit to data. Dashed line indicates probable behavior discussed in text.

anomalously large, between 6 and 8 kbar. The large value of hysteresis loop width indicates that the pressure gradients in the cell containing quartz are larger than those measured in the Teflon cell used for calibration. We believe that this effect is caused by the large strength of the quartz. We therefore ignored data from the interior hysteresis loop because it was obtained over a pressure range which may have been substantially affected by incomplete pressure gradient reversals.

Upon examination at the end of the experiments, quartz samples typically showed 3–5 major fractures roughly parallel to the cylinder axis. These fractures generally initiated at the slots which contained the heater and thermocouple wires. In the experiments on glass and quartz, loud cracking noises which may have been related to the formation of these fractures were heard upon compression at pressures near 10 kbar. The fractures probably remained closed at pressures above a few kilobars and did not appreciably affect the diffusivity measurements. The two low data points at the lowest pressures (Figure 9) suggest that the fractures may have opened below a few kilobars pressure.

From the data in Figure 9 the nominal 1-bar value of the diffusivity for quartz is  $0.031 \text{ cm}^2 \text{ s}^{-1}$ , and the rate of increase with pressure is  $1.7\% \text{ kbar}^{-1}$ . The 1-bar value is within the range of values of diffusivity which can be calculated from thermal conductivity data given by Clark [1966, p. 466]. These values range from  $\kappa = 0.029$  to  $\kappa = 0.033 \text{ cm}^2 \text{ s}^{-1}$  (with the reported values of Clark interpolated to  $40^\circ\text{C}$ — $K = 0.0145 \text{ cal cm}^{-1} \text{ s}^{-1} \text{ }^\circ\text{C}^{-1}$  and  $0.0157 \text{ cal cm}^{-1} \text{ s}^{-1} \text{ }^\circ\text{C}^{-1}$ , respectively—and with the assumptions that  $\rho = 2.65 \text{ g/cm}^3$  and  $c = 10.9 \text{ cal/mol } ^\circ\text{K}$ ). The rate of increase of diffusivity with pressure is equivalent to an increase of conductivity of  $1.2 \times 10^{-4} \text{ cal}$

$\text{cm}^{-1} \text{ s}^{-1} \text{ kbar}^{-1}$ , in excellent agreement with the value  $1.3 \times 10^{-4} \text{ cal cm}^{-1} \text{ s}^{-1} \text{ kbar}^{-1}$  reported by Schloessin and Beck [1970].

**Sodium chloride.** Sodium chloride was ground into a fine powder and pressed, slightly damp, to 14 kbar to form a sample of 97% theoretical density. It was not possible to form a single sample of 5.08 cm (2.0 inches) in length, so the final sample was composed of two shorter segments. The thermocouple broke during this run at an applied pressure of 20 kbar during the first increase in pressure, so the four data points which were obtained were corrected to a final pressure by subtracting 3 kbar from the pressure applied to the piston. This value of the half-hysteresis width was observed in all of our experiments (except those on quartz) in which one or more hysteresis loops were obtained. The four data points give a diffusivity of  $0.031 \text{ cm}^2 \text{ s}^{-1}$  at 1 bar ( $40^\circ\text{C}$ ) and a rate of increase of diffusivity with pressure of  $3.2\% \text{ kbar}^{-1}$  to 18 kbar. The 1-bar value of the diffusivity is close to the value of  $0.029 \text{ cm}^2 \text{ s}^{-1}$ , which can be calculated from published values of thermal conductivity data [Clark, 1966, p. 465].

**Silica glass.** The diffusivity was measured on samples of homogeneous silica glass to 35 kbar (Figure 10). Upon examination after the experiments the samples typically showed 3–5 major fractures similar to those observed in quartz. If a linear fit is made to the data to 35 kbar, the diffusivity is given by  $\kappa(\text{cm}^2 \text{ s}^{-1}) = 0.0068 - 6.7 \times 10^{-6}P(\text{kbar})$ . The zero-pressure value agrees with that which can be calculated from the thermal conductivity data of Ratcliffe [1959]. Note that the diffusivity of silica glass decreases with pressure, in contrast to the diffusivity of its crystalline counterpart, quartz, which increases with pressure. The data show a systematic departure from the straight line fitted to the data, being consistently low in the ~15- to ~25-kbar region and then rising with further increase in pressure.

**Comparison with theory.** An approximate expression for the pressure dependence of the thermal diffusivity has been given by Fujisawa *et al.* [1968]:

$$\frac{\kappa}{\kappa_0} \sim \left(\frac{B}{B_0}\right)\left(\frac{v_m}{v_{m0}}\right) \sim \left[1 + \frac{P}{B_0} \left(\frac{dB}{dP}\right)_0\right] \cdot \left[1 + \frac{P}{v_{m0}} \left(\frac{dv_m}{dP}\right)_0\right] \quad (5)$$

where  $B(\text{kbar})$  is the bulk modulus,  $v_m(\text{km/s})$  is the phonon velocity, and the subscript 0 refers to the values of these quantities at 1-bar pressure. Values of the parameters required in this equation are listed in Table 1. In the case of NaCl, for which  $(dv_m/dP)_0$  is known, the last term of this equation contributes less than 10% to the calculated change of diffusivity. The values of this derivative are not known for the other substances; however, they are likely to be of the same magnitude as for NaCl, so the lack of knowledge of this term does not seriously affect the approximation.

TABLE 1. Parameters for Equation (5)

Substance	$B_0$ , kbar	$dB/dP$	$v_{m0}$ , km s <sup>-1</sup>	$dv_m/dP$ , km s <sup>-1</sup> kbar <sup>-1</sup>	Predicted Change in $\kappa$ , % kbar <sup>-1</sup>	Observed Change in $\kappa$ , % kbar <sup>-1</sup>
NaCl	245	5.3	2.9	$1.5 \times 10^{-2}$	+2.5	+3.2
Quartz	374	6.4	4.5	...	+1.7	+1.7
Silica	370	-7.3	4.1	...	-4.0	-0.1

All data are from Clark [1966] except  $dB/dP$  and  $dv_m/dP$ , which are from Roberts and Ruppini [1971] and Fujisawa *et al.* [1968], respectively.

The values of  $\kappa$  predicted by (5) are in good agreement with the measured values for quartz and sodium chloride (Table 1). Equation 5 also correctly predicts the decrease of diffusivity for fused silica but severely overestimates its magnitude. The decrease of diffusivity with pressure is associated with the anomalous bulk modulus derivative, which is characteristic of fused silica and Pyrex glass but not of most other glasses [e.g., Birch, 1966]. We therefore expect that the negative pressure dependence of diffusivity is characteristic of silica glass and will not be found in glasses which do not have anomalous bulk modulus derivatives. From (5), however, we see that this decrease will persist only in that range of pressures where the bulk modulus is behaving anomalously. At high pressures the glass 'stiffens,' and the diffusivity should increase with pressure. Our data suggest that this reversal in gradient occurs at  $\sim 25$  kbar. It is worth noting that Bridgman's [1924] measurements of thermal conductivity for Pyrex glass, which has a negative, but smaller, bulk modulus derivative than fused silica, show that the conductivity increases slightly with pressure. Since  $K = \kappa\rho c$ , this observation suggests that if the predicted small diffusivity decrease occurs, it is offset by the density increase.

#### CONCLUSIONS: SUMMARY OF DATA

The pressure dependence of the thermal diffusivity at 40°C for the substances studied may be represented as follows ( $\kappa$  in square centimeters per second,  $P$  in kilobars):

Teflon I-II, $P < 5.5$ kbar	$\kappa = 0.0012 + 3.6 \times 10^{-5}P$
Teflon III, $5.5 \text{ kbar} < P < 35$ kbar	$\kappa = 0.0012 + 8.0 \times 10^{-5}P$
Quartz, perpendicular to $c$ axis, $P \leq 30$ kbar	$\kappa = 0.031 + 5.3 \times 10^{-4}P$
NaCl (polyxl), $P \leq 18$ kbar	$\kappa = 0.031 + 9.5 \times 10^{-4}P$
Silica glass, $P \leq 36$ kbar	$\kappa = 0.0068 - 6.7 \times 10^{-5}P$

The thermal conductivity of Teflon I-II is approximately constant to 5.5 kbar, in the range 0.0075–0.0078 cal/cm s° C. Above 5.5 kbar the conductivity of Teflon III is given by

$$K = 0.0062 + 4.0 \times 10^{-5}P$$

The specific heat of Teflon decreases with pressure and is discontinuous across the Teflon II-III phase change.

**Acknowledgments.** We thank J. Yamane, L. Faus, and J. DeGrosse for fabricating the many intricate parts for the experiments. S. Bailey Brown aided with data reduction, and B. Gola provided invaluable continuous encouragement. This research was funded by National Science Foundation grant GA-31897. Publication 1486 of the Institute of Geophysics and Planetary Physics, University of California, Los Angeles.

#### REFERENCES

Andersson, P., and G. Bäckström, Specific heat of solids at high pressures from simultaneous measurements of thermal conductivity and diffusivity, *High Temp. High Pressures*, **4**, 101, 1972.

- Birch, F., Compressibility: Elastic constants, *Geol. Soc. Amer. Mem.* **97**, 97, 1966.
- Bridgman, P. W., The thermal conductivity and compressibility of several rocks under high pressures, *Amer. J. Sci.*, **7**, 81, 1924.
- Bridgman, P. W., The resistance of nineteen metals to 30,000 kg/cm<sup>2</sup>, *Proc. Amer. Acad. Arts Sci.*, **72**, 157, 1938.
- Bridgman, P. W., Rough compressions of 177 substances to 40,000 kg/cm<sup>2</sup>, *Proc. Amer. Acad. Arts Sci.*, **76**, 1948.
- Carlsaw, H. S., and J. C. Jaeger, *Conduction of Heat in Solids*, 2nd ed., 510 pp., Oxford University Press, New York, 1959.
- Clark, S. P., Thermal conductivity, *Geol. Soc. Amer. Mem.* **97**, 459, 1966.
- Davidson, T. E., and A. P. Lee, The study of the structural and transformation characteristics of the pressure-induced polymorphs in bismuth, *Trans. Met. Soc. AIME*, **230**, 1035, 1964.
- Fujisawa, H., N. Fujii, H. Mizutani, H. Kanamori, and S. Akimoto, Thermal diffusivity of Mg<sub>2</sub>SiO<sub>4</sub>, Fe<sub>2</sub>SiO<sub>4</sub>, and NaCl at high pressures and temperatures, *J. Geophys. Res.*, **73**, 4727, 1968.
- Heydemann, P. L. M., The Bi I-II transition pressure measured with a dead-weight piston gauge, *J. Appl. Phys.*, **38**, 2640, 1967. (Correction, *J. Appl. Phys.*, **38**, 3424, 1967.)
- Jaeger, J. C., The uses of complete temperature-time curves for determination of thermal conductivity with particular reference to rocks, *Aust. J. Phys.*, **12**, 203, 1959.
- Jaeger, J. C., and J. H. Sass, A line-source method for measuring the thermal conductivity and diffusivity of cylindrical specimens of rock and other poor conductors, *Brit. J. Appl. Phys.*, **15**, 1187, 1964.
- Kirichenko, Yu. A., B. N. Oleinik, and T. Z. Chadovich, Thermal properties of polymers, *J. Eng. Phys.*, **7**(5), 70, 1964.
- Mooney, D. L., and R. G. Steg, Pressure dependence of the thermal conductivity and ultrasonic attenuation of non-metallic solids, *High Temp. High Pressure*, **1**, 237, 1969.
- Ozawa, T., and K. Kanari, Thermal conductivity of polytetrafluoroethylene, *J. Polym. Sci., Part B*, **5**, 771, 1967.
- Pistorius, C. W. F. T., Transitions and melting of polytetrafluoroethylene (Teflon) under pressure, *Polymer*, **5**, 315, 1964.
- Ratcliffe, E. H., Thermal conductivities of fused and crystalline quartz, *Brit. J. Appl. Phys.*, **10**, 22, 1959.
- Rigby, H. A., and C. W. Bunn, A room-temperature transition in polytetrafluoroethylene, *Nature*, **164**, 583, 1949.
- Roberts, R. W., and R. Rupp, Volume dependence of the Grüneisen parameter of alkali halides, *Phys. Rev., Ser. B*, **4**, 2041, 1971.
- Schloessin, H. H., and A. E. Beck, On the pressure and temperature dependence of the lattice thermal conductivity of enstatite, silica, and pyrophyllite, *Eos Trans. AGU*, **51**, 420, 1970.
- Schloessin, H. H., and Z. Dvorak, Anisotropic lattice thermal conductivity in enstatite as a function of pressure and temperature, *Geophys. J. Roy. Astron. Soc.*, **27**, 499, 1972.
- Shelley, D. L., and S. F. Huber, Thermal diffusivity of poly (tetrafluoroethylene) between -140 and 125°C, in *Thermal Conductivity, Proceedings of the Eighth Conference*, edited by C. Y. Ho and R. E. Taylor, p. 1067, Plenum, New York, 1968.
- Weir, C. E., Temperature dependence of compression of linear high polymers at high pressure, *J. Res. Nat. Bur. Stand.*, **53**, 245, 1954.

(Received July 28, 1975;  
revised February 6, 1976;  
accepted February 20, 1976.)